International Journal of Thermophysics, Vol. 13, No. 1, 1992

Subsecond Thermophysics Research at the Boris Kidrich Institute Vincha[1]

K. D. Maglić[2] and A. S. Dobrosavljević[2]

In the early eighties, at the Boris Kidrich Institute Vincha, a method for measuring specific heat and electrical resistivity of electrical conductors in the millisecond resolution range was developed for measurements from room temperature to 1900 K. Over a period of nearly 10 years, the method was applied to different materials, including pure metals, ferrous, and nickel/chromium alloys, and to the characterization of candidate materials for thermophysical property reference standards. This paper describes the method and reviews the results obtained in specific heat and electrical resistivity studies of ferromagnetic and other materials. The paper also demonstrates capabilities of the method for describing phase transitions or anomalies in pure metals (Fe, Co, Ni) or alloys (Nichrome, austenitic stainless steel).

KEY WORDS: electrical resistivity; high-speed measurements; high temperature; phase transitions; specific heat.

1. INTRODUCTION

A subsecond technique for measuring specific heat and electrical resistivity of solid conductors was developed at the Boris Kidrich Institute (BKI) in the early eighties [1]. The method was introduced with the purpose of enabling fast and productive measurements in the range between 300 and 1900 K. This range covers the region of moderate temperature techniques as well as the higher-temperature calorimetry techniques (1000–1500 K), a temperature range for which the least number of specific heat data exists. The method is a variant of the high-temperature pulse technique developed earlier at the National Institute of Standards and Technology (NIST)

[1] Paper presented at the Second Workshop on Subsecond Thermophysics, September 20–21, 1990, Torino, Italy.

[2] Boris Kidrich Institute of Nuclear Sciences Vincha, Beograd, Yugoslavia.

0195-928X/92/0100-0003$06.50/0

(1500–4000 K) [2] and at the Instituto di Metrologia "G. Colonnetti" (IMGC) (1000–4000 K) [3], which was adapted for application below the radiation thermometry range, i.e., from room temperature to the limits of platinum/rhodium thermometry (1900 K).

In the past decade, the method was used for measuring specific heat and electrical resistivity for a range of electrical conductors, which include high-purity ferromagnetic metals—iron [4], nickel [5], and cobalt [6]; thermophysical property reference materials (RM)—electrolytic iron [4], POCO graphite [7], copper [8], and austenitic stainless steel [9]; and other alloys of scientific or application interest—microalloyed steel [10], Nichrome 5 [11], etc. The method was also applied with success in the study of magnetic and/or structural transitions in ferromagnetic metals [4–6] and in investigations of anomalies in the nickel-based alloys [9, 11].

The objective of this paper is to review the results obtained in specific heat and electrical resistivity studies of ferromagnetic and other materials and to demonstrate application of the method for describing and studying phase transitions or anomalies in pure metals or alloys.

2. EXPERIMENTAL

2.1. Method

The method is based on the fast electroresistive self-heating of the sample to some predetermined maximum temperature not exceeding 1900 K. Data on the sample current (I), the voltage drop across the measurement zone (U), and the emf (E) of the thermocouple located at the center of the effective sample measurement zone are collected during heating and the initial part of the cooling period. The specific heat (C_p) and electrical resistivity (ρ) of the sample are computed from these data, based on the energy balance of the effective sample volume. The heating rates (up to $1500\ \mathrm{K \cdot s^{-1}}$), the sample geometry, and the high vacuum make radiative heat loss the only significant energy loss from the effective sample volume.

The power balance for the effective part of the sample during the heating period is

$$UI = mC_p \left(\frac{dT}{dt}\right)_h + P_r \tag{1}$$

where T is the temperature of the sample, t is the time, and m is the mass of the effective sample volume. The radiated power, P_r, is given as

$$P_r = \varepsilon\sigma A(T^4 - T_a^4) \tag{2}$$

where T_a is the ambient temperature, ε is the total hemispherical emissivity, A is the effective surface area, and σ is the Stefan–Boltzmann constant. During the initial part of the cooling period, the power balance is given by

$$-mC_p\left(\frac{dT}{dt}\right)_c = P_r \tag{3}$$

where the subscripts h and c refer to the heating and cooling periods, respectively. From Eq. (1) the specific heat is obtained as

$$C_p = \frac{UI - P_r}{m(dT/dt)_h} \tag{4}$$

The total hemispherical emissivity at a specific temperature is calculated from Eqs. (1) and (3) as

$$\varepsilon = \frac{UI}{\sigma A(T^4 - T_a^4)[1 - (dT/dt)_h/(dT/dt)_c]} \tag{5}$$

The specific electrical resistivity (ρ) is determined from the electrical resistance of the sample as

$$\rho = \frac{U}{I}\frac{S}{l_e} \tag{6}$$

where S is the sample cross-sectional area and l_e is the effective sample length between the potential leads.

2.2. Measurement System

The measurement system, shown schematically in Fig. 1, consists of an experimental chamber, an electric power circuit, the measuring and control instruments, a computer system, a fast data-acquisition system, and other I/O devices.

The sample is in the form of a wire 1.5–2.5 mm in diameter, with a total length not exceeding 250 mm (the graphite sample was 6.35 mm in diameter). Three 0.05- or 0.1-mm thermocouples are fixed along the 20-mm-long central effective portion of the sample at 10-mm separations. Depending on the temperature range, K-type or S-type thermocouples are used. The center thermocouple monitors the sample temperature, while two other thermocouples check the temperature uniformity along the measuring zone. Their positive legs are also used as potential leads to measure the voltage drop across the effective measurement zone of the sample.

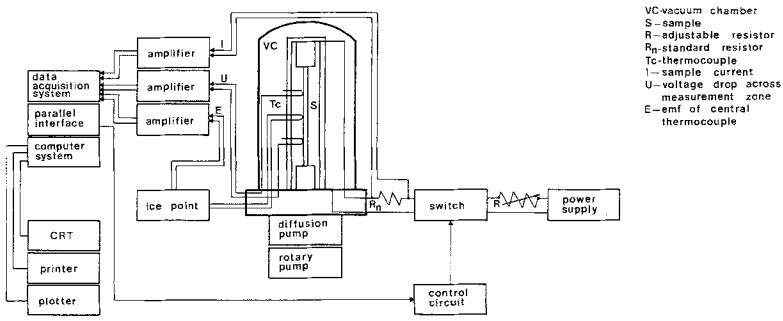

Fig. 1. Schematic of the measurement system.

The sample is mounted in the vacuum chamber between clamping electrodes, and the measurements are performed in a vacuum of 10^{-3} Pa in order to prevent oxidation of the sample. An expansion joint allows for the axial expansion of the sample during heating.

The current pulse circuit consists of a bank of several 12-V batteries connected in series or in parallel, an adjustable resistor (R), a standard resistor (R_n), and a switching unit connected in series to the sample. The adjustable resistor, which consists of several Kanthal strips, is used to control the heating rate of the sample, whereas a standard 1-mΩ resistor is used to measure the pulse current generated by the computer-controlled switching unit.

A computer performs the experimental procedure, consisting of data acquisition, control of the current pulse, and subsequent data processing. The fast 12-bit data acquisition system collects data on the sample current, the voltage drop across the effective sample length, and the thermocouple emf. The data are collected during the heating of the sample and during the initial cooling period, at a 1-kHz sampling rate.

As might be concluded from the foregoing, the method is simple and the measurement is straightforward. The difficulties arise from the need to measure the sample temperature by thermocouples in the presence of heavy current flow and from the thermal inertia of thermocouples as temperature measuring devices.

Irrespective of the thermocouple type used, the beaded thermocouple or the intrinsically welded one, there is always a certain axial displacement (Δl) between the points of contact of thermoelectrodes with the sample, causing a voltage drop (ΔE) along this distance. This voltage drop is superimposed on the thermocouple emf, causing a positive or negative error in temperature measurement. Compensation of the error from this source is based on the relation between the principal quantities measured during the heating period (I, U, E) and the electrical resistivity of the sample (ρ).

Idealized diagrams of the current, voltage drop, and thermocouple output (E) as a function of time are given in Fig. 2. The error due to the voltage drop (ΔE) is visible on the thermocouple signal, decreasing the true thermal emf (E_t) shown by the dashed line in Fig. 2c. If n data points are collected per channel during the heating period, then in the case of the ith data point, the thermocouple voltage output is

$$E(i) = E_t(i) - \Delta E(i) \tag{7}$$

Based on Fig. 2, the error voltage can be expressed as a voltage drop along the length Δl by

$$\Delta E(i) = \frac{I(i)\,\rho(i)\,\Delta l}{S} \tag{8}$$

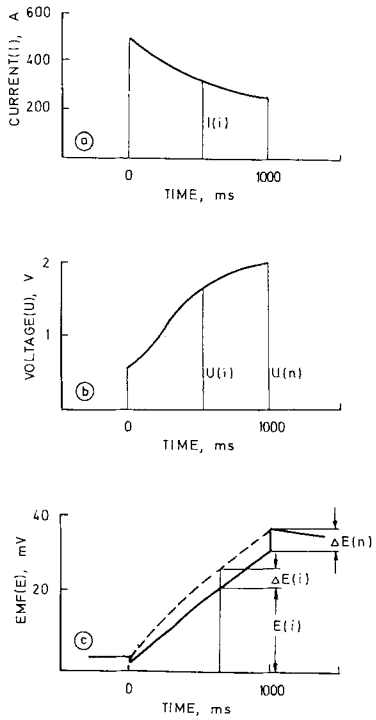

Fig. 2. Schematic of recorded signals, (a) current I, (b) voltage drop U, and (c) thermocouple output E, as functions of time t.

and since the electrical resistivity at the ith instant of time is

$$\rho(i) = \frac{U(i)}{I(i)} \frac{S}{l_e} \tag{9}$$

Eqs. (8) and (9) yield

$$\Delta E(i) = U(i) \frac{\Delta l}{l_e} \tag{10}$$

Since the ratio $\Delta l/l_e$ can be taken as constant in the whole temperature range, then

$$\frac{\Delta E(n)}{U(n)} = \frac{\Delta E(i)}{U(i)} = \text{const.} \qquad (i = 1, 2, ..., n) \tag{11}$$

Hence,

$$\Delta E(i) = U(i) \frac{\Delta E(n)}{U(n)}, \qquad (i = 1, 2, ..., n) \tag{12}$$

Thus the error $\Delta E(i)$ is determined from the corresponding value of the voltage drop $U(i)$, the value of the voltage drop at the end of the heating period $U(n)$, and the corresponding error value $\Delta E(n)$. The latter is determined as the difference between the first thermocouple reading in the cooling period and the last reading in the heating period. From Eqs. (7) and (12) the expression for the true thermal emf (E_t) at any instant during the heating period is

$$E_t(i) = E(i) + U(i) \frac{\Delta E(n)}{U(n)}, \qquad (i = 1, 2, ..., n) \tag{13}$$

The thermal inertia of thermocouples is minimized by using intrinsically attached 0.05-mm (exceptionally, 0.1-mm-)-diameter K-type or S-type thermocouple wires. Intrinsic attachment of the thermocouple wires to the sample gives better dynamic response characteristics, causes less damage to the sample, and least distorts its temperature field.

Evaluation of the method is given in detail in Ref. 12. The maximum measurement uncertainties are established at 3 and 1%, for specific heat and electrical resistivity, respectively. These uncertainties are larger in the range of phase transitions.

Talking generally about the method, it may be summarized that it is versatile with regard to the type of electrical conductors to which it can be applied, the heating rates, and the temperature range of coverage, from

room temperature to any temperature below melting point up to 1900 K. The apparatus can be relatively simple and inexpensive. It may consist of a simple vacuum chamber with clamping electrodes, which permits installation of 200-mm-long samples, and with an expansion joint that allows for the expansion of the sample at high temperature. The pulse circuit requires several 12-V batteries and a simple switching circuit consisting of high-current contactors. Control of the measurement, data acquisition, and data processing may be performed on a personal computer. Sample fabrication is simple and permits quick and easy installation and work.

3. RESULTS

The materials which were the subject of subsecond thermal physics research at BKI can be grouped into three main categories: (i) the high-purity ferromagnetic materials, (ii) the thermophysical property reference materials (candidates or established reference materials), and (iii) other materials, e.g., special steels and NiCr alloys.

Table I. Summary of Experiments

Material	Ref. No.	Number of experiments performed	Temperature range (K)		
			Specific heat	Elèctrical resistivity	Emissivity
1. Ferromagnetic materials					
Iron	4	48	350–1750	350–1750	1000–1750
Cobalt	6	21	350–1700	300–1700	1040–1580
Nickel	5	10	350–1500	350–1500	1000–1700
2. Reference materials					
Iron	4, 19	48	350–1750	350–1750	1000–1750
POCO AXM-5Q1 graphite	7, 19	51	350–1500	350–1750	900–1680
St. 1.4970	9	14	325–1500	300–1500	1320–1490
Copper RM-5	8, 19	12	350–1300	300–1350	1020–1330
3. Other materials					
Nichrome 5	11	7	350–1500	320–1500	1150–1450
Niomol 490	10	9	325–1500	325–1500	1180–1450

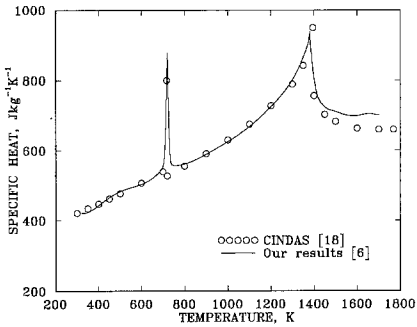

Fig. 3. Specific heat of cobalt [6].

3.1. Ferromagnetic Metals

From this group three metals were studied extensively: electrolytic iron (99.9% purity), supplied by NIST as standard reference material (NIST SRM 1463); cobalt (99.999% purity), manufactured by Johnson & Matthey Chemicals Limited, U.K., and nickel (99.999% purity), also manufactured by Johnson & Matthey Chemicals Limited, U.K. In Table I, the performed measurements and the temperature ranges covered for these three materials are given.

Figure 3 shows the specific heat versus temperature function obtained for cobalt, and Fig. 4 presents the electrical resistivity data for the same material. It is interesting that both the specific heat and the electrical resistivity measurements performed on cobalt (Johnson & Matthey) detected the magnetic transition 15 K lower than is usually quoted in the literature or in data tables and that the same lower transition temperature

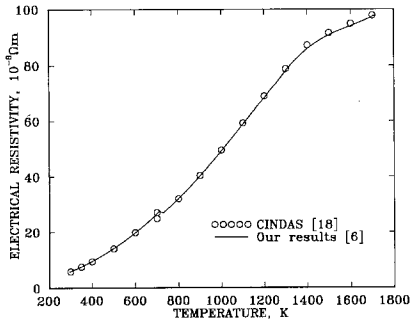

Fig. 4. Electrical resistivity of cobalt [6].

was confirmed in the thermal diffusivity measurements [6] on high-purity cobalt from the same manufacturer.

Additional details concerning our experimental results for iron, cobalt, and nickel are given in the papers cited above.

3.2. Thermophysical Property Reference Materials

A group of materials was investigated in order to establish their specific heat and electrical resistivity versus temperature functions, as a part of different round-robin programs. The aim of these cooperative measurements was to establish, confirm, and/or extend their range of application as thermophysical property standard reference materials (SRMs). They include the already-mentioned electrolytic iron (NIST SRM), POCO AXM-5Q1 graphite (NIST SRM), austenitic stainless steel St. 1.4970 (DKG Arbeitskreiss Thermophysik SRM), and high-purity polycrystalline copper (NIST Research Material). For the first three, which are in fact thermal conductivity reference materials, the measured specific heat data represented component information for computing thermal conductivity functions from the experimentally determined thermal diffusivity data. Basic information describing our experiments on the above-mentioned thermophysical property reference materials is also included in Table I.

As shown in Fig. 5, our specific heat data (300–1500 K) obtained for POCO AXM-5Q1 graphite NIST thermophysical property SRM [7] is in good agreement with the medium temperature data (400–100 K) of Taylor and Groot [13] and smoothly joins the high-temperature pulse calorimetry data (1500–3000 K) of Cezairliyan and Miiller [14], providing a continuous set, from room temperature to 3000 K.

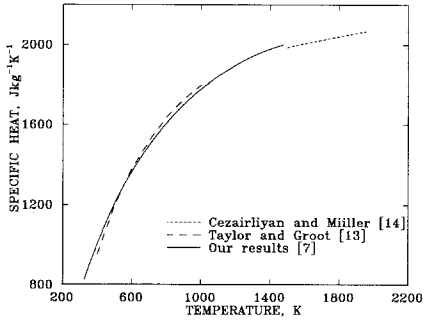

Fig. 5. Specific heat of POCO AXM-5Q1 graphite [7].

Austenitic stainless steel St. 1.4970 was among the first of the materials selected by the "Thermophysics Working Group" of the German Ceramic Society (DKG) as candidates for their thermophysical property SRMs. Our measurements joined a round-robin series in progress, after six data sets by other authors already existed. Subsequent evaluation of these data, together with the two additional data sets of Binkele [15], gave a recommended function in excellent agreement with our results, except in the anomaly region, where our pulse measurements were too fast for the sluggish nature of this anomaly, shifting it some 50 K higher.

Parallel specific heat measurements were performed on copper (NIST Research Material 5 Copper Heat Capacity Test Specimen) at NIST by drop calorimetry [16] and at BKI by the millisecond-resolution pulse method [8]. The aim of these measurements was to provide reliable experimental information, which might ultimately lead to extending the application of copper as a calorimetry reference material above room temperature. As can be seen from Fig. 6, the agreement between the two sets of results is good and they joint smoothly with the set of data chosen by Osborne and Kirby [17] for the range below 300 K.

3.3. Other Materials

Recent measurements on Nichrome 5 [11] and the microalloyed steel Niomol 490 [10] have confirmed the applicability of our pulse method to the study of different materials for which information on specific heat is important for scientific and application purposes. Our measurements on Nichrome 5, a well-known electroresistive and thermoelectric alloy, provided information of importance for understanding the nature of the anomaly occurring in this material above 800 K and for its possible use as

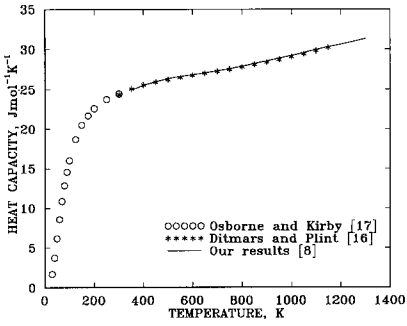

Fig. 6. Heat capacity of copper research material RM-5 [8].

Table II. Phase Transitions Studied in Iron [4], Cobalt [6], and Nickel [5]

Material	Ref. No.	Type of transition	Transition temperature (K)	
			Recommended	Detected
Iron	4	Magnetic	1043	1043
Iron	4	bcc–fcc	1185	1200
Iron	4	fcc–bcc	1667	1664
Cobalt	6, 20	hcp–fcc	715	720
Cobalt	6, 20	Magnetic	1395	1380
Nickel	5	Magnetic	625	624

an encapsulating material for drop calorimetry. The specific heat and electrical resistivity studies of Niomol 490 were undertaken to provide necessary information for welding of complex structures made of this material. Table I summarizes the number of experiments and the temperature range covered for the above two materials.

4. DETECTION AND STUDY OF PHASE TRANSITIONS

Our millisecond pulse method of measuring specific heat and electrical resistivity proved suitable for the study of all transitions in metals and alloys occurring sufficiently fast as not to be affected by the heating rates between 500–1500 $K \cdot s^{-1}$ typically for this method. Table II presents information on the transitions studied in three ferromagnetic materials—iron [4], cobalt [6], and nickel [5]—including a comparison between the critical transition temperatures determined by our measurements and the corresponding recommended values [18]. As an example, Fig. 7 illustrates the

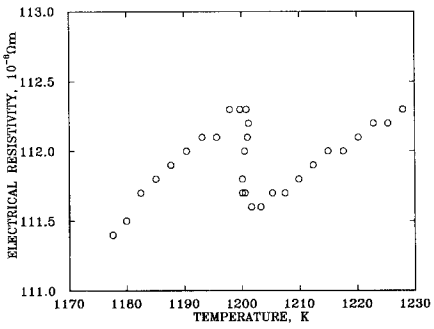

Fig. 7. Electrical resistivity of iron in the region of the α–γ phase transition [4].

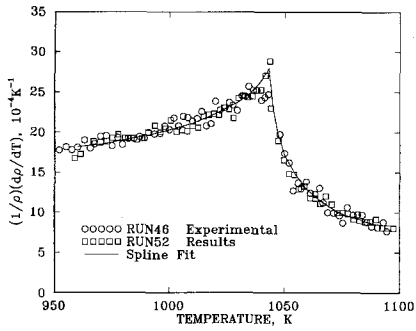

Fig. 8. The first derivative of the electrical resistivity function in the region of the magnetic phase transition of iron [19].

effect of the α–γ transformation in iron [4] on the electrical resistivity function. The magnetic transition of iron is manifested by a wide peak, both in the first derivative of electrical resistivity (Fig. 8) and in the specific heat function (Fig. 9) [19].

For the study of sluggish transitions, another method, with controlled, relatively slow sample temperature change was developed. This method gave good results in the study of the hcp–fcc transition in cobalt [20].

5. CONCLUSIONS

Extensive studies of specific heat and electrical resistivity of electrical conductors—ferromagnetic metals, thermal property reference materials, or

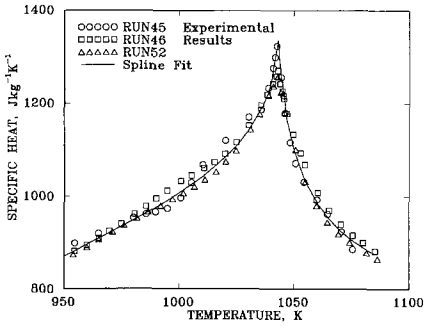

Fig. 9. Specific heat of iron in the region of the magnetic phase transition [19].

other metals and alloys—performed at BKI using subsecond calorimetry provided a number of reliable and interesting results.

The millisecond pulse method used for these measurements has fulfilled expectations with respect to its efficiency, reliability, and accuracy. It might be stated that, after nearly a decade of its use and improvements, the method has reached a mature state of development.

The method is versatile, permitting also computation of hemispherical total emissivity from the acquired measurement data. The accuracy of the emissivity results increases with increasing measurement temperatures, from 1000 K to the maximum operating temperature.

Plans for subsecond measurements at BKI in the near-future involve a range of materials, including refractory metals. The latter were studied extensively in the high-temperature range at NIST (formerly National Bureau of Standards), by a high-temperature variant of the present method. Planned measurements should fill the gap in the 300–1500 K range.

ACKNOWLEDGMENTS

Most of the measurements mentioned in this review have been performed as part of the cooperation in thermophysical properties research between the U.S. National Institute of Standards and Technology and the Boris Kidrich Institute Vincha, under the auspices of the USA–Yugoslav Joint Board for Scientific and Technological Cooperation. Financial support of the Joint Board is gratefully acknowledged.

REFERENCES

1. A. Dobrosavljević and K. Maglić, in *Measurement Techniques in Heat and Mass Transfer*, R. I. Soloukhin and N. H. Afgan, eds. (Hemisphere, Washington, DC, 1985), pp. 411–420.
2. A. Cezairliyan, M. S. Morse, H. A. Berman, and C. W. Beckett, *J. Res. Natl. Bur. Stand. (U.S.)* **74A**:65 (1970)
3. F. Righini, A. Rosso, and G. Ruffino, *High Temp. High Press.* **4**:597 (1972).
4. A. S. Dobrosavljević, K. D. Maglić, and N. Lj. Perović, *High Temp. High Press.* **17**:591 (1985).
5. K. D. Maglić, A. S. Dobrosavljević, and N. Lj. Perović, in *Thermal Conductivity 20*, D. P. H. Hasselman and J. R. Thomas, Jr., eds. (Plenum, New York, 1989), pp. 81–92.
6. A. S. Dobrosavljević, K. D. Maglić, and N. Lj. Perović, *High Temp. High Press.* **21**:317 (1989).
7. A. S. Dobrosavljević, N. Lj. Perović, and K. D. Maglić, *High Temp. High Press.* **19**:303 (1987).
8. A. S. Dobrosavljević and K. D. Maglić, *High Temp. High Press.* (in press).
9. A. S. Dobrosavljević and K. D. Maglić, *Int. J. Thermophys.* **13**:57 (1992).
10. A. S. Dobrosavljević and N. Lj. Perović, Personal communication.

11. K. D. Maglić, A. S. Dobrosavljević, and N. Lj. Perović, *High Temp. High Press.* (in press).
12. A. S. Dobrosavljević and K. D. Maglić, *High Temp. High Press* **21**:411 (1989).
13. R. E. Taylor and H. Groot, *High Temp. High Press.* **12**:147 (1980).
14. A. Cezairliyan and A. Miiller, *Int. J. Thermophys.* **6**:285 (1985).
15. L. Binkele, *DKG Fachausschussbericht Nr. 28, 2. Bericht des Arbeitskreises "Thermophysik"* (Deutsche Keramische Gesellschaft, Koeln, 1990), pp. 5–46.
16. D. A. Ditmars and C. A. Plint, *Int. J. Thermophys.* (in press).
18. Y. S. Touloukian and C. Y. Ho, *CINDAS Data Series on Material Properties, Vol. III-1* (McGraw–Hill, New York, 1981).
19. A. S. Dobrosavljević, Ph.D. thesis (University of Beograd, Beograd, 1989).
20. A. S. Dobrosavljević and K. D. Maglić, in *Thermal Conductivity 21*, H. A. Fine and C. J. Cramers, eds. (Plenum, New York, 1990), pp. 523–530.